Math Meth Oper Res (2013) 77:101–130
DOI 10.1007/s00186-012-0416-3

ORIGINAL ARTICLE

# Primal-dual methods for the computation of trading regions under proportional transaction costs

**Roland Herzog · Karl Kunisch · Jörn Sass**

Received: 28 February 2012 / Accepted: 19 September 2012 / Published online: 18 October 2012


**Abstract** Portfolio optimization problems on a finite time horizon under proportional transaction costs are considered. The objective is to maximize the expected utility of the terminal wealth. The ensuing non-smooth time-dependent Hamilton–Jacobi–Bellman equation is solved by regularization and the application of a semi-smooth Newton method. Discretization in space is carried out by finite differences or finite elements. Computational results for one and two risky assets are provided.

**Keywords** Portfolio optimization · Transaction costs · Complementarity problem · Semi-smooth Newton method · Augmented Lagrangian method

Roland Herzog: This research was carried out in part at the Johann Radon Institute for Computational and Applied Mathematics (RICAM), Austrian Academy of Sciences, Linz, Austria; Karl Kunisch: Research supported in part by the Fonds zur Förderung der wissenschaftlichen Forschung (FWF) under SFB 32, Mathematical Optimization and Applications in the Biomedical Sciences; Jörn Sass: J. Sass gratefully acknowledges financial support by Deutsche Forschungsgemeinschaft (DFG).

R. Herzog (✉)
Faculty of Mathematics, Chemnitz University of Technology, 09107 Chemnitz, Germany
e-mail: roland.herzog@mathematik.tu-chemnitz.de
URL: http://www.tu-chemnitz.de/herzog

K. Kunisch
Institute for Mathematics and Scientific Computing, Karl Franzens University Graz,
Heinrichstrasse 36, 8010 Graz, Austria
e-mail: karl.kunisch@uni-graz.at
URL: http://www.kfunigraz.ac.at/imawww/kunisch

J. Sass
Department of Mathemaics, University of Kaiserslautern, P.O. Box 3049 ,
67663 Kaiserslautern, Germany
e-mail: sass@mathematik.uni-kl.de
URL: http://www.mathematik.uni-kl.de/sass/

## 1 Introduction

We consider numerical methods for the solution of a continuous-time portfolio optimization problem with a finite time horizon and under proportional transaction costs. An investor aims at maximizing the expected utility of the terminal value of the liquidated investment portfolio (wealth). The supremum of this expected value over all admissible trading strategies, the value function, satisfies a non-smooth time-dependent Hamilton–Jacobi–Bellman (HJB) equation of the form

$$\max\{V_t + \mathcal{L}V,\ \max_{1\le i\le n} \mathcal{L}_{B_i} V,\ \max_{1\le i\le n} \mathcal{L}_{S_i} V\} = 0, \tag{1.1}$$

cf. Akian et al. (1995) for a finite-time horizon and Davis and Norman (1990), Shreve and Soner (1994), Akian et al. (1996) for an optimization problem with infinite time horizon. The latter leads to a stationary problem (no dependency on time).

In our case, (1.1) is posed on the so-called solvency region $\mathcal{S}$ times the time interval $(0, T)$ and it is endowed with appropriate boundary and terminal conditions. The number $n$ denotes the number of risky assets (stocks) in the portfolio. While $\mathcal{L}$ is a second-order differential operator, the buy and sell operators $\mathcal{L}_{B_i}$ and $\mathcal{L}_{S_i}$ are of first order.

The sought-after optimal trading strategy is determined in terms of the time-dependent partitioning of the solvency region $\mathcal{S}$ into subregions determined by which of the $2n + 1$ terms in (1.1) are zero (active), and by the manifolds separating these subregions. These subregions, the trading regions, describe which action is optimal, e.g., if the first term $V_t(y) + \mathcal{L}V(y)$ in (1.1) is zero for a risky fraction $y$, then it is optimal not to trade. The component $y_i$ of the risky fraction $y = (y_1, \ldots, y_n)^\top$ is the proportion of wealth invested in stock $i$. This is different from the corresponding problem without costs, for which Merton (1969) showed that it is optimal to keep the risky fraction constant. This strategy requires continuous trading and cannot be followed when facing realistic transaction costs. Regions where one or several of the other operators in (1.1) are zero correspond to regions where buying or selling a particular stock is optimal. For more references and other cost structures we refer to the introductions of Irle and Sass (2006) and Zakamouline (2005). For our model with proportional costs these trading regions characterize the optimal strategy which is of the form that no trading occurs as long as the fractions invested in the stocks stay inside the no-trading (NT) region. Due to the dynamics of the stocks, these fractions might hit the boundary; then infinitesimally small trading to keep the fractions inside the NT-region is optimal, cf. (Shreve and Soner 1994, Section 9) for the stationary case.

It is the purpose of this paper to devise numerical methods for the solution of this problem, i.e. for finding the trading regions, on the basis of methods that were first analyzed for a simpler problem in Griesse and Kunisch (2009). The main idea consists of replacing (1.1) by an approximating penalty-type formulation,

$$V_t + \mathcal{L}V + c\sum_{i=1}^{n} \max\{0, \mathcal{L}_{B_i} V\} + c\sum_{i=1}^{n} \max\{0, \mathcal{L}_{S_i} V\} = 0. \tag{1.2}$$

This approach was recently used in Dai and Zhong (2010) for a similar problem. For the simpler problem $\max\{-\triangle y + f, \ |\nabla y| - g\} = 0$ it was shown in Griesse and Kunisch (2009) that the proposed penalty method is in fact regularizing and that the solutions of the penalized problems converge in appropriate function spaces to the solution of the original HJB equation. After discretization in space and time, (1.2) can be solved using a semi-smooth Newton methods, see e.g. Ito and Kunisch (2008). The latter is naturally implemented in terms of an active set strategy.

Compared to the results in Dai and Zhong (2010), in this paper we go a step beyond. In the case of one risky asset we compare the results obtained by applying a semi-smooth Newton method to both, the regularized and unregularized formulations of (1.2) to investigate the effect of the regularization parameter. In the two-dimensional case, the use of regularization appears to be numerically essential. However, it may slow down the iteration procedure and give rise to highly convective contributions from the first-order operators $\mathcal{L}_{B_i}$ and $\mathcal{L}_{S_i}$. For this reason, in addition to using upwinding techniques, we propose to combine the Newton approach with an Augmented Lagrangian concept. Differently from Dai and Zhong (2010), we use a primal-dual strategy as opposed to a purely primal one for the determination of the active sets. A further distinctive feature of the proposed algorithm is an adaptive time-stepping technique.

We mention that a different numerical approach for the stationary problem with consumption as in Davis and Norman (1990), Shreve and Soner (1994), Akian et al. (1996) was proposed in Muthuraman (2007), Muthuraman and Kumar (2006). There the authors employ a monotonically decreasing update of the no-trading region, which is motivated by a policy improvement procedure. By contrast, for our time-dependent problem we propose a Newton scheme to resolve the trading and no-trading regions in every time step. We do not need a priori structural assumptions on the location of the NT region.

Problems of the form (1.1) with different differential operators of first and second order arise frequently in stochastic control. This was pointed out, for instance in Evans (1979). In Li and Wang (2009) a HJB equation related to (1.1) arising in European stock pricing with proportional transaction costs was investigated. The authors show that for a penalty approach the viscosity solutions of the penalized problems converge to the viscosity solution of the original HJB equation as the penalty parameter tends to infinity. In Hodder et al. (2001) finite difference schemes for variational inequalities arising in international asset pricing are investigated and a time-stepping scheme based on the dynamic programming principle is proposed. An interesting model for optimal soaring is developed in Almgren and Tourin (2004). It also leads to a HJB equation of the type (1.1).

The contents of the paper are organized as follows. We summarize the necessary background on portfolio optimization in Sect. 2. In Sect. 3 we discuss and compare the regularized and unregularized approaches for the solution of (1.1) in the case of one risky asset ($n = 1$). Section 4 is devoted to the numerical treatment of the regularized problem for the case $n = 2$. Numerical examples demonstrating the performance of the algorithms are provided for both cases. In Sect. 5 we discuss some model extensions.

## 2 Background on portfolio optimization

We consider a continuous-time market model consisting of one bond or bank account and $n \geq 1$ stocks with prices $(P_0(t))_{t\in[0,T]}$ and $(P_i(t))_{t\in[0,T]}$, $i = 1, \dots, n$, respectively. For given interest rate $r \geq 0$, trend parameter $\mu \in \mathbb{R}^n$, and non-singular volatility-matrix $\sigma \in \mathbb{R}^{n\times n}$, these evolve according to

$$\begin{aligned} \mathrm{d}P_0(t) &= P_0(t)\, r\, \mathrm{d}t, & P_0(0) &= 1, \\ \mathrm{d}P_i(t) &= P_i(t)\, \mu_i\, \mathrm{d}t + P_i(t) \sum_{j=1}^{n} \sigma_{ij}\, \mathrm{d}W_j(t), & P_i(0) &= 1, \quad i = 1, \dots, n. \end{aligned}$$

Here $W = (W(t))_{t\in[0,T]}$ is an $n$-dimensional standard Brownian motion on a probability space $(\Omega, \mathcal{A}, P)$. Let $\mathcal{F} = (\mathcal{F}_t)_{t\in[0,T]}$ denote the augmented filtration generated by $W$.

### 2.1 Trading without transaction costs

Without transaction costs, trading of an investor may be described by initial capital $\overline{X}(0) > 0$ and risky fraction process $(\eta(t))_{t\in[0,T]}$, $\eta(t) = (\eta_1(t), \dots, \eta_n(t))^\top$, where $\eta_i(t)$ is the fraction of the portfolio value (wealth) which is held in stock $i$ at time $t$. The corresponding *wealth process* $(\overline{X}(t))_{t\in[0,T]}$ is defined self-financing by

$$\mathrm{d}\overline{X}(t) = \big(1 - \mathbf{1}^\top \eta(t)\big)\overline{X}(t)\, r\, \mathrm{d}t + \sum_{i=1}^{n} \eta_i(t)\, \overline{X}(t) \left( \mu_i\, \mathrm{d}t + \sum_{j=1}^{n} \sigma_{ij}\, \mathrm{d}W_j(t) \right),$$

where $\mathbf{1} = (1, \dots, 1)^\top$. In this section we call $(\eta_t)_{t\geq 0}$ *admissible* if it is adapted, measurable, bounded, and $\overline{X}(T) > 0$ holds. The terminal wealth $x = \overline{X}(T) > 0$ is evaluated by a power utility function

$$\tfrac{1}{\alpha}\, x^\alpha \quad \text{for any} \quad \alpha < 1, \quad \alpha \neq 0. \tag{2.1}$$

The parameter $\alpha$ models the preferences of an investor. The strategy for the limiting case $\alpha \to 0$ corresponds to logarithmic utility, i.e., to maximizing the expected rate of return. The case $\alpha > 0$ corresponds to less risk averse and $\alpha < 0$ to more risk averse utility functions. Merton (1969) showed that for logarithmic ($\alpha = 0$) and power utility the optimal trading strategy is given by a constant optimal risky fraction

$$\eta(t) = \hat{\eta}, \quad t \in [0, T], \quad \text{for} \quad \hat{\eta} = \frac{1}{1-\alpha} A^{-1}(\mu - r\,\mathbf{1}), \tag{2.2}$$

where $A = \sigma\sigma^\top$ denotes the covariance matrix of the stock returns.

## 2.2 Proportional transaction costs

Keeping the risky fraction constant like in (2.2) involves continuous trading. This is no longer adequate in the presence of transaction costs. We consider proportional costs $\gamma \in (0, 1)$ which correspond to the proportion of the traded volume which has to be paid as fees. These are paid from the bank account (bond).

The trading policy can be described by increasing processes $L_i = (L_i(t))_{t\in[0,T]}$ and $M_i = (M_i(t))_{t\in[0,T]}$ representing the cumulative purchases and sales of stock $i$, $i = 1, \ldots, n$. We require that $L = (L_1, \ldots, L_n)^\top$, $M = (M_1, \ldots, M_n)^\top$ are right-continuous, $\mathcal{F}$-adapted, with initial values $L(0-) = M(0-) = 0$. Since transaction fees are paid from the bank account, the dynamics of the controlled wealth processes $(X_0(t))_{t\in[0,T]}$ and $(X_i(t))_{t\in[0,T]}$, corresponding to the amount of money in the bank account and the amount invested in stock $i$, are

$$\mathrm{d}X_0(t) = rX_0(t)\,\mathrm{d}t - (1+\gamma)\,\mathrm{d}(\mathbf{1}^\top L(t)) + (1-\gamma)\,\mathrm{d}(\mathbf{1}^\top M(t)), \tag{2.3a}$$

$$\mathrm{d}X_i(t) = X_i(t)\,\mu_i\,\mathrm{d}t + X_i(t)\sum_{j=1}^{n}\sigma_{ij}\,\mathrm{d}W_j(t) + \mathrm{d}L_i(t) - \mathrm{d}M_i(t). \tag{2.3b}$$

We write the wealth in stocks as vector $X(t) = (X_1(t), \ldots, X_n(t))^\top$.

The objective is the maximization of the expected utility at the terminal trading time $T$, over all control processes $L$ and $M$ which satisfy the conditions above and for which the wealth processes $X_i$, $i = 0, \ldots, n$, stay in the solvency region

$$\mathcal{S}^0 := \{(x_0, x) \,:\, x_0 \in \mathbb{R},\ x \in \mathbb{R}^n,\ x_0 + \mathbf{1}^\top x - \gamma\,\|x\|_1 > 0\} \tag{2.4}$$

which consists of all positions in bond and stocks for which a strictly positive wealth remains after liquidating the stock holdings. Note that in (2.4), $\gamma\,\|x\|_1 = \sum_{i=1}^n \gamma\,|x_i|$ are the liquidation costs. Starting in $(X_0(0-), X(0-) \in \mathcal{S}^0$ we thus require

$$(X_0(t), X(t)) \in \mathcal{S}^0, \quad t \in [0, T).$$

Accordingly, we consider the maximization of the expected utility of the terminal total wealth after liquidating the position in the stocks, i.e., we consider the value function

$$\begin{aligned}\Phi(t, x_0, x)\\ = \sup_{(L,M)} \mathrm{E}\big[\tfrac{1}{\alpha}\big(X_0(T) + \mathbf{1}^\top X(T) - \gamma\,\|X(T)\|_1\big)^\alpha \mid X_0(t-) = x_0, X(t-) = x\big].\end{aligned} \tag{2.5}$$

**Theorem 2.1** *The value function $\Phi$ is continuous, concave in $(x_0, x)$, and satisfies the homotheticity property*

$$\Phi(t, c\,x_0, c\,x) = c^\alpha\,\Phi(t, x_0, x) \quad \textit{for} \quad c > 0,\ t \in [0, T),\ (x_0, x) \in \mathcal{S}^0, \tag{2.6}$$

*as well as the boundary conditions*

$$\Phi(t, x_0, x) \to \begin{cases} 0, & \text{if } 0 < \alpha < 1, \\ -\infty, & \text{if } \alpha < 0. \end{cases} \quad \text{for } (x_0, x) \to (\bar{x}_0, \bar{x}) \in \partial\mathcal{S}^0. \tag{2.7}$$

*Further, $\Phi$ is a viscosity solution of*

$$\max\{\Phi_t + \mathcal{A}\Phi, \max_{1\le i\le n} \mathcal{A}_{B_i}\Phi, \max_{1\le i\le n} \mathcal{A}_{S_i}\Phi\} = 0 \qquad \text{on } [0, T) \times \mathcal{S}^0, \tag{2.8}$$

$$\Phi(T, x_0, x) = \tfrac{1}{\alpha}\left(x_0 + \mathbf{1}^\top x - \gamma\, \|x\|_1\right)^\alpha \qquad \text{for } (x_0, x) \in \mathcal{S}^0, \tag{2.9}$$

*where the differential operators $\mathcal{A}$ (generator of $(X_0, X)$) and $\mathcal{A}_{B_i}$, $\mathcal{A}_{S_i}$, $i = 1, \ldots, n$, are defined by*

$$\mathcal{A}h(x_0, x) = r\, x_0\, h_{x_0}(x_0, x) + \sum_{i=1}^n \mu_i\, x_i h_{x_i}(x_0, x) + \tfrac{1}{2}\sum_{i,j=1}^n A_{i,j}\, x_i\, x_j\, h_{x_i,x_j}(x_0, x),$$
$$\mathcal{A}_{B_i}h(x_0, x) = -(1+\gamma)\, h_{x_0}(x_0, x) + h_{x_i}(x_0, x),$$
$$\mathcal{A}_{S_i}h(x_0, x) = (1-\gamma)\, h_{x_0}(x_0, x) - h_{x_i}(x_0, x)$$

*for all smooth functions $h$.*

*Proof* The proof can be carried out similarly as in Akian et al. (1996) or Shreve and Soner (1994), even if we consider a finite time horizon problem and consequently a time-dependent value function. In particular the first part is standard, corresponding to (Shreve and Soner 1994, Propositions 3.1–3.3). Continuity of $\Phi$ in $t$ can be shown using the no-trading strategy and the optimal strategy without costs to derive lower and upper bounds for the change of the value function in time. The convergence in (2.7) follows from arguments as used in (Shreve and Soner 1994, Corollaries 5.5, 5.8) and the fact that $\Phi$ is a viscosity solution follows along the lines of (Shreve and Soner 1994, Sections 6), only that we need the continuity of $\Phi$ in $t$ as well. □

Depending on which of the three terms in the outer max operation in (2.8) is active at a given $(t, x_0, x) \in [0, T] \times \mathcal{S}^0$, i.e., equals 0, we say that $(t, x_0, x)$ belongs to the no-trading region, or the buy or sell region, respectively. More precisely, at time $t$, we define the buy regions, sell regions and the no-trading region as follows:

$$B_i^0(t) = \{(x_0, x) \in \mathcal{S}^0 \;:\; \mathcal{A}_{B_i}\Phi(t, x_0, x) = 0\},$$
$$S_i^0(t) = \{(x_0, x) \in \mathcal{S}^0 \;:\; \mathcal{A}_{S_i}\Phi(t, x_0, x_1) = 0\},$$
$$NT^0(t) = \mathcal{S}^0 \setminus \bigcup_{1\le i\le n} (B_i^0(t) \cup S_i^0(t)).$$

The boundaries between these sets determine the optimal trading policy.

## 2.3 Reduction of the dimension

It is convenient to consider the risky fraction process rather than the wealth process (2.3). For wealth $x_i$ in stock $i$ and total wealth $\xi = x_0 + \mathbf{1}^\top x$, the risky fractions are given by $y_i = \frac{x_i}{\xi}$, $i = 1, \ldots, n$.

From the homotheticity property (2.6) of $\Phi$ we deduce

$$\Phi(t, x_0, x) = \xi^\alpha \Phi\left(t, \tfrac{x_0}{\xi}, \tfrac{x_1}{\xi}, \ldots, \tfrac{x_n}{\xi}\right). \tag{2.10}$$

Thus it is enough to consider

$$V(t, y) = \Phi(t,\ 1 - \mathbf{1}^\top y,\ y), \quad y \in \mathcal{S}, \tag{2.11}$$

where

$$\mathcal{S} = \{y \in \mathbb{R}^n\ :\ \gamma\, \|y\|_1 < 1\} \tag{2.12}$$

is the solvency region in terms of the risky fractions. For $\Phi(t, x_0, x) = \xi^\alpha V(t, x/\xi)$, we obtain under suitable differentiability assumptions

$$\Phi_t = \xi^\alpha V_t, \quad \Phi_{x_0} = \xi^{\alpha-1}\left(\alpha V - y^\top V_y\right), \quad \Phi_{x_i} = \xi^{\alpha-1}\left(\alpha V + (\mathrm{e}_i - y)^\top V_y\right),$$
$$\Phi_{x_i,x_j} = \xi^{\alpha-2}\left(\alpha(1-\alpha)V + (\alpha-1)(\mathrm{e}_i + e_j - 2y)^\top V_y + (\mathrm{e}_i - y)^\top V_{yy}(e_j - y)\right),$$

where $V_y$ and $V_{yy}$ denote the gradient and the Hessian of $V$, and $\mathrm{e}_1, \ldots, \mathrm{e}_n$ are the unit vectors in $\mathbb{R}^n$. We get for $y = x/\xi$

$$\Phi_t(t, x_0, x) = \xi^\alpha V_t(t, y), \quad \mathcal{A}\Phi(t, x_0, x) = \xi^\alpha \mathcal{L}V(t, y),$$
$$\mathcal{A}_{B_i}\Phi(t, x_0, x) = \xi^{\alpha-1}\mathcal{L}_{B_i}(t, y)V, \quad \mathcal{A}_{S_i}\Phi(t, x_0, x) = \xi^{\alpha-1}\mathcal{L}_{S_i}V(t, y).$$

For classical solutions for which the above derivatives exist and are continuous, Theorem 2.1 carries over directly to Theorem 2.2 below. For a viscosity solution $\Phi$ it can be shown that also $V$ is a viscosity solution of (2.14), which then yields Theorem 2.2, cf. (Shreve and Soner 1994, Proposition 8.1):

**Theorem 2.2** *The value function $V$ is continuous and concave in $y$ with*

$$V(t, y) \to \begin{cases} 0, & \text{if } 0 < \alpha < 1 \\ -\infty, & \text{if } \alpha < 0 \end{cases} \quad \text{for } \to \bar{y} \in \partial\mathcal{S}, \quad t \in (0, T). \tag{2.13}$$

*Further, $V$ is a viscosity solution of*

$$\max\{V_t + \mathcal{L}V,\ \max_{1\le i\le n} \mathcal{L}_{B_i}V,\ \max_{1\le i\le n} \mathcal{L}_{S_i}V\} = 0 \tag{2.14}$$

*on* $[0, T) \times \mathcal{S}$ *with terminal condition*

$$V(T, y) = \tfrac{1}{\alpha}(1 - \gamma\, \|y\|_1)^\alpha, \quad y \in \mathcal{S}. \tag{2.15}$$

*The operators in* (2.14) *are defined by*

$$\begin{aligned}\mathcal{L}V &= \alpha\Big(r + (\mu - r\mathbf{1})^\top y - \tfrac{1}{2}(1-\alpha)\, y^\top A\, y\Big)\, V \\ &\quad + \Big[\big(\mathrm{diag}(\mu - r\mathbf{1}) - (\mu - r\mathbf{1})^\top y\, I\big)\, y \\ &\quad - \tfrac{1}{2}(1-\alpha)\sum_{i,j=1}^{n} A_{ij}\, y_i\, y_j (\mathrm{e}_i + \mathrm{e}_j - 2y)\Big]^\top V_y \\ &\quad + \tfrac{1}{2}\sum_{i,j=1}^{n} A_{ij}\, y_i\, y_j (\mathrm{e}_i - y)^\top V_{yy} (\mathrm{e}_j - y), \qquad (2.16a)\\ \mathcal{L}_{B_i} V &= -\alpha\,\gamma\, V + (\mathrm{e}_i + \gamma\, y)^\top V_y, \quad i = 1, \ldots, n, \qquad (2.16b)\\ \mathcal{L}_{S_i} V &= -\alpha\,\gamma\, V - (\mathrm{e}_i - \gamma\, y)^\top V_y, \quad i = 1, \ldots, n. \qquad (2.16c)\end{aligned}$$

The trading regions are now given by

$$\begin{aligned}B_i(t) &= \{y \in \mathcal{S} \,:\, \mathcal{L}_{B_i} V(t, y) = 0\},\\ S_i(t) &= \{y \in \mathcal{S} \,:\, \mathcal{L}_{S_i} V(t, y) = 0\},\\ NT(t) &= \mathcal{S} \setminus \bigcup_{1 \le i \le n} (B_i(t) \cup S_i(t)).\end{aligned}$$

They correspond to buying stock $i$, selling stock $i$ and not trading at all. On

$$\bigcap_{1\le i\le n} R_i, \quad R_i \in \{B_i, S_i\},$$

we thus get from $\mathcal{L}_{R_i} V = 0,\ i = 1, \ldots, n$, that

$$V(t, y) = C_{R_1,\ldots,R_n}(t)\left(1 + \sum_{i=1}^{n} \gamma_i\, y_i\right)^{\alpha}, \qquad (2.17)$$

where $\gamma_i = \gamma$ if $R_i = B_i$ and $\gamma_i = -\gamma$ if $R_i = S_i$.

*Remark 2.3* Based on Theorem 2.1 we may further analyze the regularity of the value function and the properties of the trading regions. From the results in Shreve and Soner (1994) and the numerical analysis in Akian et al. (1996), Dai and Zhong (2010); Muthuraman and Kumar (2006) we expect the value function $\Phi = \Phi(t, x_0, x)$ to be continuously differentiable in $t$ and in $x_0$, and twice continuously differentiable in $x = (x_1, \ldots, x_n)^\top$ for $(t, x_0, x) \in (0, T) \times \big(\mathcal{S}^0 \setminus \{(x_0, x_1, \ldots x_n) \,|\, x_i = 0 \text{ for some } i\}\big)$. For $n = 1$ see Dai and Yi (2009). However, their proof based on a double-obstacle problem may not carry over to $n > 1$. Smoothness of $\Phi$ would carry over to $V$.

In the following we shall assume uniqueness of the viscosity solutions of (2.8), (2.9) and thus of (2.14), (2.15). For a sketch of a proof in the setting of no borrowing and no short selling, we refer to Akian et al. (1995), which carries over to the original setting in Theorem 2.1 for $0 < \alpha < 1$. Typically, the case $\alpha < 0$ is more difficult since then the utility function is unbounded near 0. Further we assume that $NT^0(t) \neq \emptyset$ for all $t \in [0, T)$. Due to the homotheticity property (2.6) the trading regions for the original problem are cones. Therefore, $NT^0(t) \neq \emptyset$ implies $NT(t) \neq \emptyset$ for all $t \in [0, T)$.

### 2.4 Numerical treatment of portfolio optimization as a non-variational complementarity problem

It should be recognized that, even in the stationary case with $V_t$ not appearing in (2.14), this problem is not of variational type. It is thus distinct from the obstacle problem, not only since the constraints involve spatial derivatives of the state, rather than the state itself, but also since it cannot be interpreted in a straightforward way as the necessary optimality condition of a minimization problem in function space. In a function space setting such problems have received very little attention. In Griesse and Kunisch (2009) we investigated

$$\begin{aligned} &\max\{-\triangle u - f, \quad |\nabla u| - g\} = 0 \quad \text{a.e. in } \Omega, \\ &u = 0 \quad \text{on } \Gamma = \partial\Omega, \end{aligned} \tag{2.18}$$

where $\Omega \subset \mathbb{R}^d$ is a bounded domain with smooth boundary $\Gamma$, as a prerequisite to the present work. There we mainly investigated two approaches, namely of (2.18) as a complementarity problem, which involves the introduction of a new variable $\lambda$ for the term $|\nabla u| - g$, and alternatively a regularization procedure, which realizes the constraint on $|\nabla u| - g$ by means of a penalty formulation. The complementarity approach was already treated in Kunisch and Sass (2007) for the one-dimensional case of (2.14). The introduction of the regularization term allows to interpret the approach as a semi-smooth Newton method in function spaces, whereas without the regularization the interpretation as semi-smooth Newton method is only possible after discretization. This is described in more detail in Sect. 3.1 below.

## 3 The case of one risky asset

In the case of only one risky asset (stock) $n = 1$, Eq. (2.14) reduces to

$$\max\{V_t + \mathcal{L}V,\ \mathcal{L}_B V,\ \mathcal{L}_S V\} = 0 \quad \text{on } (0, T) \times \mathcal{S} \tag{3.1}$$

on $\mathcal{S} = (-1/\gamma, 1/\gamma)$ with boundary conditions

$$V(t, -1/\gamma) = V(t, 1/\gamma) = \begin{cases} 0, & \text{if } 0 < \alpha < 1 \\ -\infty, & \text{if } \alpha < 0 \end{cases} \quad \text{for all } t \in (0, T) \tag{3.2}$$

and terminal condition on $\mathcal{S}$

$$V(T, y) = \tfrac{1}{\alpha}(1 - \gamma\, \|y\|_1)^\alpha. \tag{3.3}$$

By (2.16), the linear differential operators in (3.1) become

$$\mathcal{L}V = \big[\alpha\,(r + (\mu - r)\,y) + \tfrac{1}{2}\alpha\,(\alpha - 1)\,\sigma^2 y^2\big]V \\ + \big[(\mu - r)\,y\,(1-y) + (\alpha - 1)\,\sigma^2 y^2 (1-y)\big]V_y + \tfrac{1}{2}\sigma^2 y^2 (1-y)^2\,V_{yy} \tag{3.4a}$$

$$\mathcal{L}_B V = (1 + \gamma\,y)\,V_y - \alpha\,\gamma\,V \tag{3.4b}$$

$$\mathcal{L}_S V = -(1 - \gamma\,y)\,V_y - \alpha\,\gamma\,V. \tag{3.4c}$$

## 3.1 Regularization

Instead of treating (3.1)–(3.3) directly, we consider the regularized formulation

$$V_t + \mathcal{L}V + c\,\max\{0, \mathcal{L}_B V\} + c\,\max\{0, \mathcal{L}_S V\} = 0 \tag{3.5}$$

with regularization parameter $c > 0$ and subject to the boundary and terminal conditions (3.2)–(3.3). The motivation for introducing this formulation for the numerical realization of (3.1) resides in the fact that we shall utilize a Newton type method. Clearly this is impeded by the max-operation appearing in (3.1). The regularized form (3.5), however, lends itself to a semi-smooth Newton treatment. To briefly explain this point for a significantly simpler problem which,we consider

$$\begin{aligned} &\max\{-\triangle u - f, \quad u' - g, \quad h - u'\} = 0 \quad \text{a.e. in } \Omega, \\ &u = 0 \quad \text{on } \partial\Omega, \end{aligned} \tag{3.6}$$

and the family of regularized problems:

$$-\triangle u + c\,\max\{0, u' - g\} + c\,\max\{0, h - u'\} = f \quad \text{in } \Omega, \quad u = 0 \quad \text{on } \partial\Omega. \tag{3.7}$$

Above $\Omega$ is an interval in $\mathbb{R}$, and $f$, $g$ and $h$, with $g \geq h$ are given. Setting $\lambda = f + \triangle u$ this equation can be expressed as

$$\begin{aligned} F(\lambda) := \lambda - c\,\max\{0, \big((-\triangle)^{-1}(f - \lambda)\big)' - g\} \\ -c\,\max\{0, h - \big((-\triangle)^{-1}(f - \lambda)\big)'\} = 0, \end{aligned} \tag{3.8}$$

where $\triangle^{-1}$ denotes the solution operator for the Laplacian in $\Omega$ with homogenous Dirichlet boundary conditions. It can be shown that for any $c > 0$ the mapping $F$ is Newton differentiable from $L^2(\Omega)$ to itself, and consequently the semi-smooth Newton algorithm applied to $F(\lambda) = 0$ converges locally $q$-superlinearly to the solution $u_c$ of (3.7), see Griesse and Kunisch (2009), for example.

Clearly, the choice of the regularization parameter $c$ must be addressed. In practice this will frequently be done heuristically, but for the related class of optimal control problems with pointwise constraints, path-following algorithms were developed in Hintermüller and Kunisch (2006) which allow self-tuning of the regularization parameter $c$.

### 3.2 Discretization in time

For the numerical realization a semi-discretization of (3.5) backwards in time by the one-step $\theta$ method with $\theta \in (0, 1]$ is used. Let $V^n$ denote the unknown at time level $n$. Then $V^n$ is computed from $V^{n+1}$ according to

$$\frac{V^{n+1} - V^n}{\tau} + \mathcal{L}(\theta\, V^n + (1-\theta)\, V^{n+1}) + c\, \max\{0, \mathcal{L}_B(\theta\, V^n + (1-\theta) V^{n+1})\} + c\, \max\{0, \mathcal{L}_S(\theta\, V^n + (1-\theta) V^{n+1})\} = 0 \tag{3.9}$$

subject to the boundary conditions (3.2). The time step size is denoted by $\tau$. For the specific choices $\theta = 1$ and $\theta = 1/2$ the scheme becomes the implicit (backward) Euler and the Crank-Nicolson methods, respectively.

### 3.3 Semi-smooth Newton method

At any given time level $n$, (3.9) represents a second-order elliptic partial differential equation for the variable $V^n$ with a non-smooth first-order term. The nonsmoothness arises from the presence of the $\max\{0, \cdot\}$ operation. However, this operation enjoys the Newton differentiability property, which allows for the formulation of a generalized Newton's method. A Newton derivative of $\max\{0, \mathcal{L}_B V\}$ is given by the indicator function of $\{\mathcal{L}_B V > 0\}$. The structure of the indicator function entails that the Newton step takes the form of an active set method. This has been rigorously proved in Griesse and Kunisch (2009) for a similar problem setting.

Apart from the $\max\{0, \cdot\}$ terms, (3.9) is a linear equation. Hence the Newton step, written in terms of the new iterate $V = V^n_{k+1}$ is given by

$$\frac{V^{n+1} - V}{\tau} + \mathcal{L}(\theta\, V + (1-\theta) V^{n+1}) + c\, \chi_{A^B_k} \mathcal{L}_B(\theta\, V + (1-\theta) V^{n+1}) + c\, \chi_{A^S_k} \mathcal{L}_S(\theta\, V + (1-\theta) V^{n+1}) = 0, \tag{3.10}$$

subject to the boundary conditions (3.2), where

$$\begin{aligned} A^B_k &= \{y \in (-1/\gamma, 1/\gamma) : \mathcal{L}_B(\theta\, V^n_k + (1-\theta) V^{n+1}) > 0\} \\ A^S_k &= \{y \in (-1/\gamma, 1/\gamma) : \mathcal{L}_S(\theta\, V^n_k + (1-\theta) V^{n+1}) > 0\}. \end{aligned} \tag{3.11}$$

The complete semi-smooth Newton (SSN) algorithm is given as Algorithm 3.1. An initial guess for $V^n_0$ on the current time level is obtained from linear extrapolation of $V^{n+1}$ and $V^{n+2}$, i.e.,

$$V^n_0 = 2\, V^{n+1} - V^{n+2}, \tag{3.12}$$

or $V^{N-1}_0 = V^N$ in case of the first time step.

### 3.4 Discretization in space and treatment of boundary conditions

The spatial operators in (3.10)–(3.11) are discretized by finite differences. The trading bounds $\sup B(t)$ and $\inf S(t)$ lie to the left and right of the Merton fraction, see (2.2),

$$\hat{\eta} = \frac{1}{1-\alpha}\frac{\mu - r}{\sigma^2}.$$

In order to resolve the trading bounds accurately, a refined grid in $[\hat{\eta}-1, \hat{\eta}+1]$ around the Merton fraction and a coarse grid away from it on $[-1/\gamma, \hat{\eta}-1]$ and $[\hat{\eta}+1, 1/\gamma]$ was used. For $\hat{\eta} \in (0, 1)$ this choice guarantees that the $NT$-region is covered by the refined grid. For $\hat{\eta}$ far away from 0 it might happen that it does not lie in the $NT$-region, see e.g., Irle and Sass (2006), Shreve and Soner (1994), and the choice for the grid would have to be adapted.

The second derivative $V_{yy}$ was discretized by the standard stencil $[1 \;\; -2 \;\; 1]/h^2$. The convective terms involving $\mathcal{L}_B$ and $\mathcal{L}_S$ in (3.10) need to be stabilized. For this purpose upwind differences for $V_y$ were utilized. That is, $V_y$ in $\mathcal{L}_B V$ was discretized by first-order backward differences, while $V_y$ in $\mathcal{L}_S V$ was approximated by forward differences. The same discretization was used to determine the active sets in (3.11).

The boundary conditions (3.2) for the Newton step (3.10) read

$$V^n(-1/\gamma) = V^n(1/\gamma) = \begin{cases} 0, & \text{if } 0 < \alpha < 1 \\ -\infty, & \text{if } \alpha < 0 \end{cases}$$

and thus they require special care if $\alpha < 0$. Regardless of the sign of $\alpha$ we shall exploit the fact that the buy and sell trading regions extend to the boundaries $-1/\gamma$ and $1/\gamma$, respectively. This follows from the boundary conditions (2.13) with arguments as used to derive the corresponding Corollaries 8.7/8.8 in Shreve and Soner (1994). That is, the solution of the continuous problem satisfies $\mathcal{L}_B V(t, y) = 0$ for $y$ near $-1/\gamma$ at all times $t \in [0, T)$, i.e.,

$$V(t, y) = c_B(t)(1 + \gamma\, y)^\alpha$$

holds with an unknown integration constant $c_B(t) \neq 0$.

Suppose that $a \in (-1/\gamma, \sup B(t))$ is a given number in the buy region. From $\mathcal{L}_B V(t, a) = 0$ we infer

$$(1 + \gamma\, a)\, V_y(t, a) - \alpha\, \gamma\, V(t, a) = 0. \tag{3.13a}$$

Similarly, we obtain for $b \in (\inf S(t), 1/\gamma)$ the condition

$$-\,(1 + \gamma\, b)\, V_y(t, b) - \alpha\, \gamma\, V(t, b) = 0. \tag{3.13b}$$

Thus using the Robin boundary conditions (3.13) allows us to solve the Newton step (3.10) on the subdomain $(a, b) \subset (-1/\gamma, 1/\gamma)$ only. We refer to this as the *reduced domain* technique and it leads to a significant reduction of the size of the computational domain. The unknown constants $c_B(t)$ and similarly $c_S(t)$ can be computed a posteriori from

$$c_B(t) = V(t, a)(1 + \gamma\, a)^{-\alpha}, \quad c_S(t) = V(t, b)(1 - \gamma\, b)^{-\alpha}. \tag{3.14}$$

The solution $V(t,\cdot)$ can thus be recovered outside $(a,b)$. Note that this procedure can be used regardless of the sign of $\alpha$.

For convenience, we summarize the semi-smooth Newton time-stepping method as Algorithm 3.1.

**Algorithm 3.1** Semi-smooth Newton time-stepping method in the one-dimensional case

Initialize $V^N$ according to (3.3)
**for** $n = N-1, \dots, 1$ **do**
  Initialize $V_0^n := 2\,V^{n+1} - V^{n+2}$ (or $V_0^{N-1} = V^N$) and set $k := 0$
  **while** not converged (SSN) **do**
    Set

$$A_k^B := \{y \in (-1/\gamma, 1/\gamma) : \mathcal{L}_B(\theta\, V_k^n + (1-\theta)V^{n+1}) > 0\}$$
$$A_k^S := \{y \in (-1/\gamma, 1/\gamma) : \mathcal{L}_S(\theta\, V_k^n + (1-\theta)V^{n+1}) > 0\}$$

    Solve for $V_{k+1}^n$

$$\frac{V^{n+1} - V}{\tau} + \mathcal{L}(\theta\, V + (1-\theta)V^{n+1}) + c\,\chi_{A_k^B}\mathcal{L}_B(\theta\, V + (1-\theta)V^{n+1}) + c\,\chi_{A_k^S}\mathcal{L}_S(\theta\, V + (1-\theta)V^{n+1}) = 0.$$

    either on the full domain $(-1/\gamma, 1/\gamma)$ with boundary conditions (3.2), or on the reduced domain $(a,b)$ with boundary conditions (3.13)
    **if** reduced domain case **then**
      Compute $c_B$ and $c_S$ from (3.14)
      Set $V_{k+1}^n := \begin{cases} c_B(1+\gamma\,y)^\alpha & \text{on } (-1/\gamma, a) \\ c_S(1-\gamma\,y)^\alpha & \text{on } (b, 1/\gamma) \end{cases}$
    **end if**
    Increase $k$
  **end while** (SSN)
  Set $V^n := V_k^n$
**end for**

### 3.5 Unregularized active set method

For comparison, we also implemented an unregularized version of the semi-smooth Newton iteration. It is based on the following reformulation of (3.1) as a complementarity problem:

$$\begin{aligned} &V_t + \mathcal{L}V + \lambda_B + \lambda_S = 0 \\ &\lambda_B \geq 0, \quad \mathcal{L}_B V \leq 0, \quad \lambda_B\,\mathcal{L}_B V = 0 \\ &\lambda_S \geq 0, \quad \mathcal{L}_S V \leq 0, \quad \lambda_S\,\mathcal{L}_S V = 0 \end{aligned} \tag{3.15}$$

with boundary and terminal conditions (3.2)–(3.3). Using the $\max\{0,\cdot\}$ complementarity function, (3.15) can be equivalently expressed as

$$\begin{aligned} &V_t + \mathcal{L}V + \lambda_B + \lambda_S = 0 \\ &\lambda_B = \max\{0, \lambda_B + \varrho\,\mathcal{L}_B V\}, \quad \lambda_S = \max\{0, \lambda_S + \varrho\,\mathcal{L}_S V\} \end{aligned} \tag{3.16}$$

for any $\varrho > 0$. This leads to the following semidiscrete formulation of (3.1)

$$\begin{aligned} &\frac{V^{n+1}-V^n}{\tau} + \mathcal{L}(\theta\, V^n + (1-\theta)\, V^{n+1}) + \lambda_B + \lambda_S = 0 \\ &\lambda_B = \max\{0, \lambda_B + \varrho\, \mathcal{L}_B V^n\}, \quad \lambda_S = \max\{0, \lambda_S + \varrho\, \mathcal{L}_S V^n\} \end{aligned} \tag{3.17}$$

on $(0, T) \times (-1/\gamma, 1/\gamma)$. We suppose again that the active sets

$$\begin{aligned} A^B &= \{y \in (-1/\gamma, 1/\gamma) : \lambda_B + \varrho\, \mathcal{L}_B V^n > 0\} \\ A^S &= \{y \in (-1/\gamma, 1/\gamma) : \lambda_S + \varrho\, \mathcal{L}_S V^n > 0\} \end{aligned}$$

are intervals of the form $(-1/\gamma, a)$ and $(b, 1/\gamma)$. As in (3.13), we impose Robin boundary conditions at $y = a$ and $y = b$ and solve

$$\frac{V^{n+1}-V^n}{\tau} + \mathcal{L}(\theta\, V^n + (1-\theta)\, V^{n+1}) = 0 \quad \text{on } (a, b).$$

The equations in (3.17) are coupled through the active sets. Their iterative solution by Newton's method leads to Algorithm 3.2. Note that the interval structure of the active sets is enforced in step 8. The initialization of $\lambda_{B,0}^{N-1}$ and $\lambda_{S,0}^{N-1}$ in step 5 is motivated by the update formula for $\lambda_B$ and $\lambda_S$ as applied in step 12, under the best available guess $V^{N-1} = V^N$.

### 3.6 Numerical results

For all computations, a uniform time grid with 200 points with implicit Euler time-stepping ($\theta = 1$) was used. In order to resolve the trading bounds accurately, a refined grid with 4,000 grid points in $[\hat{\eta} - 1, \hat{\eta} + 1]$ around the Merton fraction and a coarse grid with 100 points each away from it on $[-1/\gamma, \hat{\eta} - 1]$ and $[\hat{\eta} + 1, 1/\gamma]$ was used. For all examples, the Robin-type boundary conditions (3.13) were employed on the reduced domain $(a, b) = \left(-\frac{1}{10\gamma}, \frac{1}{10\gamma}\right)$.

The iteration for a given time level $n$ (see steps 4–12 in Algorithm 3.1) was terminated as soon as one of the following criteria was satisfied:

(1) the active sets coincided: $A_{k+1}^B = A_k^B$ and $A_{k+1}^S = A_k^S$
(2) the time step residual

$$\left\| \max\left\{ \frac{V^{n+1}-V_{k+1}^n}{\tau} - \mathcal{L}(\theta\, V_{k+1}^n + (1-\theta)V^{n+1}),\ \mathcal{L}_B V_{k+1}^n,\ \mathcal{L}_S V_{k+1}^n \right\} \right\|_{L^\infty(\mathcal{S})} \tag{3.18}$$

after step 10 was below $10^{-7}$,
(3) the terms determining the change of active sets

$$\begin{aligned} j_B &:= \mathcal{L}_B(\theta\, V_{k+1}^n + (1-\theta)V^{n+1}) \\ j_S &:= \mathcal{L}_S(\theta\, V_{k+1}^n + (1-\theta)V^{n+1}) \end{aligned} \tag{3.19}$$

after step 10 satisfied

$$|j_B| < 10^{-6} \quad \text{on} \;\; A_k^B \setminus A_{k+1}^B \;\; \text{and on} \;\; A_{k+1}^B \setminus (A_k^B \cup A_k^S)$$
$$|j_S| < 10^{-6} \quad \text{on} \;\; A_k^S \setminus A_{k+1}^S \;\; \text{and on} \;\; A_{k+1}^S \setminus (A_k^B \cup A_k^S).$$

In all examples, criteria (1) or (3) were always satisfied first.

**Algorithm 3.2** Unregularized semi-smooth Newton time-stepping method in the one-dimensional case

1: Initialize $V^N$ according to (3.3)
2: Set

$$a := \min\left\{y \in (-1/\gamma, 1/\gamma) : \mathcal{L}V^N \geq 0\right\}$$
$$b := \max\left\{y \in (-1/\gamma, 1/\gamma) : \mathcal{L}V^N \geq 0\right\}$$

3: **for** $n = N-1, \ldots, 1$ **do**
4: Initialize $V_0^n := 2\,V^{n+1} - V^{n+2}$ (or $V_0^{N-1} = V^N$) and set $k := 0$
5: Initialize $\lambda_{B,0}^n := 2\,\lambda_B^{n+1} - \lambda_B^{n+2}$ and $\lambda_{S,0}^n := 2\,\lambda_S^{n+1} - \lambda_S^{n+2}$ or

$$\lambda_{B,0}^{N-1} := -\mathcal{L}V^N \quad \text{on } (-1/\gamma, a)$$
$$\lambda_{S,0}^{N-1} := -\mathcal{L}V^N \quad \text{on } (b, 1/\gamma)$$
$$\lambda_{B,0}^{N-1} := \lambda_{S,0}^{N-1} := 0 \quad \text{elsewhere}$$

6: **while** not converged (SSN) **do**
7: Set

$$A_k^B := \{y \in (-1/\gamma, 1/\gamma) : \lambda_{B,k}^n + \varrho\,\mathcal{L}_B V_k^n > 0\}$$
$$A_k^S := \{y \in (-1/\gamma, 1/\gamma) : \lambda_{S,k}^n + \varrho\,\mathcal{L}_S V_k^n > 0\}$$

8: Set

$$a := \max A_k^B \quad \text{and} \quad b := \min A_k^S$$

9: Solve for $V_{k+1}^n$

$$\frac{V^{n+1} - V}{\tau} + \mathcal{L}(\theta\,V + (1-\theta)V^{n+1}) = 0$$

on $(a, b)$ with boundary conditions (3.13)
10: Compute $c_B$ and $c_S$ from (3.14)
11: Set $V_{k+1}^n := \begin{cases} c_B(1+\gamma\,y)^\alpha & \text{on } (-1/\gamma, a) \\ c_S(1-\gamma\,y)^\alpha & \text{on } (b, 1/\gamma) \end{cases}$
12: Set

$$\lambda_{B,k+1}^n := -\frac{V^{n+1} - V_{k+1}^n}{\tau} - \mathcal{L}(\theta\,V_{k+1}^n + (1-\theta)V^{n+1}) \quad \text{on } (-1/\gamma, a)$$
$$\lambda_{S,k+1}^n := -\frac{V^{n+1} - V_{k+1}^n}{\tau} - \mathcal{L}(\theta\,V_{k+1}^n - (1-\theta)V^{n+1}) \quad \text{on } (b, 1/\gamma)$$

and $\lambda_{B,k+1}^n = \lambda_{S,k+1}^n = 0$ elsewhere
13: Increase $k$
14: **end while** (SSN)
15: Set $V^n := V_k^n$, $\lambda_B^n := \lambda_{B,k}^n$ and $\lambda_S^n := \lambda_{S,k}^n$
16: **end for**

*Example 3.1* In this example we consider the following problem data

| | | | |
|---|---|---|---|
| $\alpha = 0.1$ | utility exponent | $\gamma = 1.0\,\%$ | trading costs |
| $\mu = 9.6\,\%$ | stock trend | $\sigma = 0.4$ | stock volatility |
| $r = 0.0\,\%$ | interest rate | | |

on the time interval (0, 1). The Merton fraction for this example is $\hat{\eta} = 2/3$, and we consider the case with liquidation costs.

We report on the performance of Algorithm 3.1 in a MATLAB implementation with various choices of the regularization parameter $c$, see Table 1. The plot of the trading region boundaries is shown in Fig. 1. The run-time was never more than 7 seconds on a contemporary PC.

The area between the black and the red curve is the no-trading region $NT$. If at time $t$ a fraction $y \in NT(t)$ of our wealth is invested in the stocks, we would not trade. Below from the black curve we have the buy region $B$, above from the red curve the sell region $S$. Starting with a risky fraction in $NT$ we actually only touch the boundary of $B$ or $S$ as described in the introduction. But starting at $t \in [0, T)$ with a risky fraction in the interior of $B(t)$ or $S(t)$, it would be optimal to buy or sell, respectively, in such a way that after trading the new risky fraction lies on the boundary of $NT(t)$ and afterwards to continue as above.

The financial interpretation of the shape of the regions in Fig. 1 is as follows: The Merton fraction $\hat{\eta} = 2/3 > 0$ indicates that it is optimal to invest in the stocks. It is desirable to stay close to $\hat{\eta}$. From Fig. 1 we learn that for positions above $\hat{\eta}$ (dashed line) it becomes more and more attractive to sell stocks (red curve) to get closer to $\hat{\eta}$, since we have to sell all stocks at terminal time anyway. On the other hand, it is always better to be 100 % invested in the bond ($y = 0$), than to have a short position in the stocks ($y < 0$). Due to the liquidation costs at terminal time we would liquidate a short position in the stocks immediately (positive black curve). If the expected gains from the stock investment are higher than the costs, we buy stocks, as is the case for $t < 0.78$ (black curve strictly positive). The influence of these small realistic costs of

**Table 1** Performance of Algorithm 3.1 for Example 3.1 with implicit Euler time-stepping ($\theta = 1$) for various values of the regularization parameter $c$

| $c$ | Iter | $\triangle b$ | $\triangle s$ | Residual |
|---|---|---|---|---|
| 1.00E0 | 319 | – | – | 4.00E−1 |
| 1.00E1 | 459 | 0.0040 | 0.0040 | 1.97E−1 |
| 1.00E2 | 524 | 0.0005 | 0.0005 | 4.15E−2 |
| 1.00E3 | 539 | 0.0005 | 0.0005 | 6.61E−3 |
| 1.00E4 | 543 | 0.0000 | 0.0005 | 8.15E−4 |
| 1.00E5 | 550 | 0.0005 | 0.0005 | 8.76E−5 |

'iter' refers to the total number of iterations, accumulated over all 200 time steps, and 'residual' denotes the expression in (3.18) at time $t = 0$. Moreover, '$\triangle b$' denotes the shift of the computed *buy* trading boundary at time $t = 0$, compared to the previous value of $c$. It is a multiple of the local mesh size 0.0005. '$\triangle s$' is the same for the *sell* trading boundary

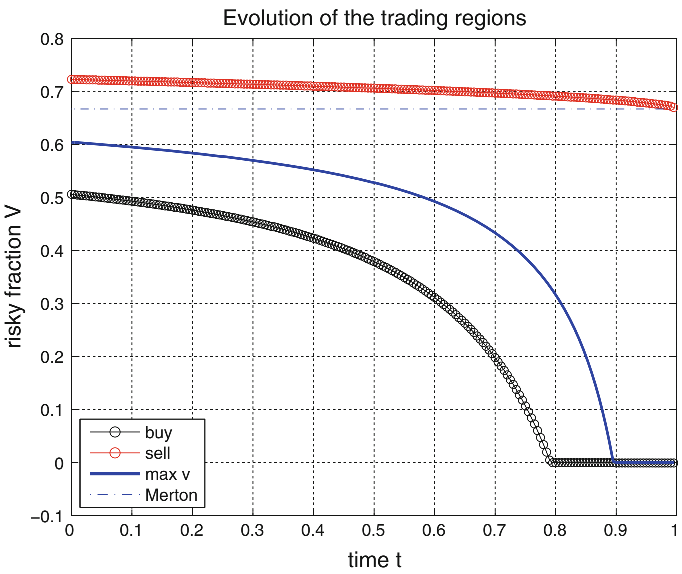


**Fig. 1** Boundaries of the trading regions in Example 3.1 (*red* and *black*). The figure also shows the Merton fraction (*dash-dotted*) and the risky fraction where $V$ assumes its maximum at any given time (*solid line*). (Color figure online)

$\gamma = 1\,\%$ can be seen very well from the solid blue curve which shows that it would be better to start at $t = 0.9$ with a position zero in the stocks than at the Merton fraction $\hat{\eta}$, which is optimal without costs. In the short remaining time the liquidation costs are higher than the expected proceeds from the stock investment.

In Fig. 2, the three terms in

$$\max\left\{\frac{V^{n+1}-V^n}{\tau} - \mathcal{L}(\theta\, V^n + (1-\theta)\, V^{n+1}),\quad \mathcal{L}_B V^n,\quad \mathcal{L}_S V^n\right\} = 0 \qquad (3.20)$$

are depicted in the vicinity of the trading bounds. Note that the angle of intersection between these curves is small. Hence the sensitivity of the boundaries of the trading regions with respect to the penalty parameter $c$ must be checked. To this end, the values $\triangle b$ and $\triangle s$ are included in Table 1. As can be seen, the boundaries converge as $c$ increases. Moreover, the table gives a clear indication that the residual error is linked to regularization.

For the sake of comparison, we also applied the unregularized Algorithm 3.2 for this and the following example. The reduced computational domain was chosen to be $(a, b) = \left(-\frac{1}{3\gamma}, \frac{1}{3\gamma}\right)$ in these cases. With the same stopping criteria in place and $\varrho = 10^1$, the residual error at $t = 0$ was found to be $3.47 \cdot 10^{-5}$ and $4.60 \cdot 10^{-6}$, respectively. It is thus comparable than the residuals obtained by the regularized algorithm (Algorithm 3.1) for appropriate values of $c$, compare Tables 1 and 2. A total number of 645 and 526 iterations were needed for all 200 time steps.

We also remark that the use of appropriate initialization of the Lagrange multipliers given in Step 5 of the Algorithm 3.2 as well as Step 8, which enforces the interval structure of the no-trading region, are essential.

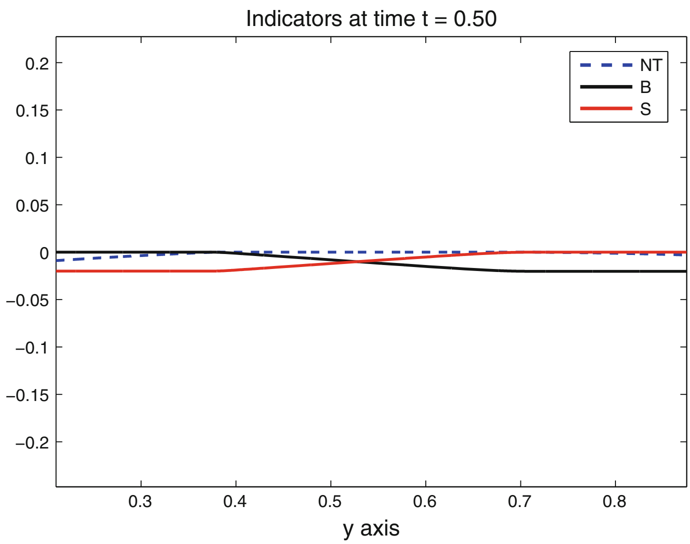


**Fig. 2** Plot of the three terms in (3.20) at $t = 0.5$ near the trading boundaries $b(t) \approx 0.38$ and $s(t) \approx 0.71$

**Table 2** Performance of Algorithm 3.1 for Example 3.2

| $c$ | Iter | $c_B$ | $c_S$ | Residual |
|---|---|---|---|---|
| 1.00E2 | 457 | −2.4561 | −1.8063 | 3.21E−1 |
| 1.00E3 | 459 | −1.0835 | −1.0474 | 1.82E−2 |
| 1.00E4 | 460 | −1.0086 | −0.9955 | 2.02E−3 |
| 1.00E5 | 462 | −1.0013 | −0.9905 | 2.18E−4 |
| 1.00E6 | 460 | −1.0006 | −0.9899 | 9.02E−5 |

See Table 1 for a legend. In addition, $c_B$ and $c_S$ denote the values of these constants, see (3.14), at time $t = 0$

*Example 3.2* Here the previous problem is modified by choosing the more risk-averse parameter

$$\alpha = -1.0 \quad \text{utility exponent.}$$

The Merton fraction is now $\hat{\eta} = 0.3$. In Fig. 3 we see that we have a similar interpretation as in Fig. 1 w.r.t. to the Merton fraction which is now smaller due to the more risk averse utility function.

We report again on the performance of Algorithm 3.1 for various choices of the regularization parameter $c$, see Table 2. As discussed before, in view of $\alpha < 0$ boundary conditions (3.13) are employed. As the reduced domain of computation, we used again $(a, b) = \left(-\frac{1}{10\gamma}, \frac{1}{10\gamma}\right)$.

*Example 3.3* In a third example, we modified Example 3.1 by choosing

$$\mu = -10.0\,\% \quad \text{stock trend.}$$

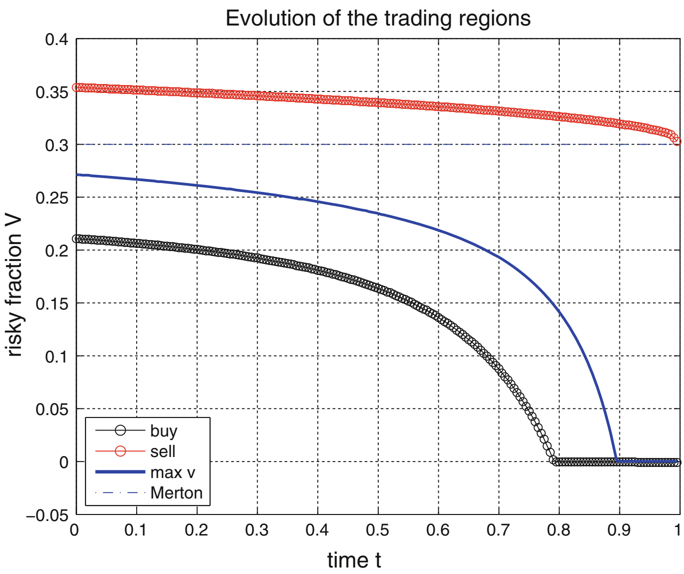


**Fig. 3** Boundaries of the trading regions in Example 3.2 (*red* and *black*). See Fig. 1 for a legend. (Color figure online)

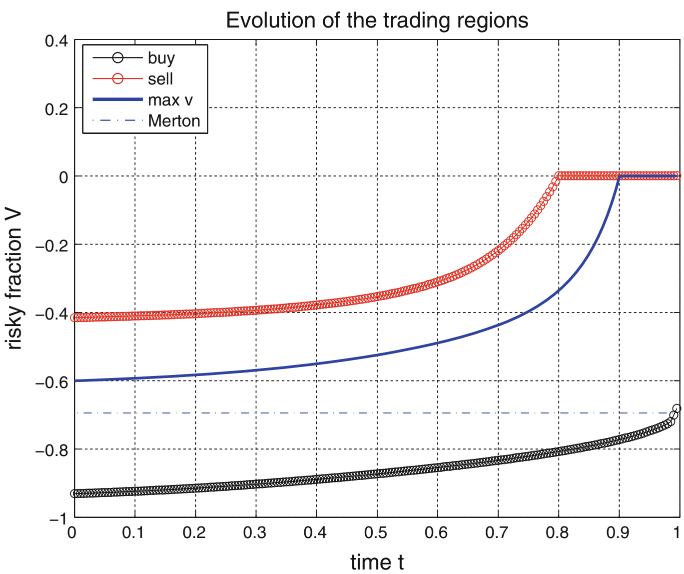


**Fig. 4** Boundaries of the trading regions in Example 3.3 (*red* and *black*). See Fig. 1 for a legend. (Color figure online)

The Merton fraction is $\hat{\eta} = -0.6944$ in this example.

In Fig. 4 we see that we have qualitatively a mirrored plot compared to Fig. 1 of Example 3.1. This is due to the fact that we now have a negative trend $\mu$ for which it can be shown that holding stocks ($y > 0$) can never be optimal. It is preferable to

**Table 3** Performance of Algorithm 3.1 for Example 3.3

| $c$ | Iter | Residual |
|---|---|---|
| 1.00E0 | 259 | 5.69E−1 |
| 1.00E1 | 367 | 2.59E−1 |
| 1.00E2 | 436 | 4.86E−2 |
| 1.00E3 | 444 | 6.83E−3 |
| 1.00E4 | 445 | 8.07E−4 |
| 1.00E5 | 446 | 8.46E−5 |

See Table 1 for a legend

be short in the stocks ($y < 0$) which allows us to profit from decreasing stock prices. Liquidation now means that we have to buy stocks at terminal time to close the short position in the stocks, and the same arguments as for the interpretation of Fig. 1 apply.

We report once again on the performance of Algorithm 3.1 for various choices of the regularization parameter $c$, see Table 3.

## 4 The case of two risky assets

In the case of two risky assets $n = 2$, the solution of Eq. (2.14) becomes significantly more involved. We recall that the solvency region

$$\mathcal{S} = \{y \in \mathbb{R}^2 \ : \ \|y\|_1 < 1/\gamma\} \tag{4.1}$$

is a diamond-shaped subset of $\mathbb{R}^2$. Parallel to the regularized formulation in the 1D case, see (3.5), we consider

$$V_t + \mathcal{L}V + c\sum_{j=1}^{2}\max\{0, \mathcal{L}_{B_j}V\} + c\sum_{j=1}^{2}\max\{0, \mathcal{L}_{S_j}V\} = 0 \tag{4.2}$$

on $[0, T) \times \mathcal{S}$ with regularization parameter $c > 0$ and subject to the boundary conditions (2.13). The terminal condition for $V$ on $\mathcal{S}$ is given by

$$V(T, y) = \tfrac{1}{\alpha}(1 - \gamma\, \|y\|_1)^{\alpha}. \tag{4.3}$$

Similar to the 1D case (3.9) we discretize (4.2) in time to obtain

$$\begin{aligned} \frac{V^{n+1} - V^n}{\tau} &+ \mathcal{L}(\theta\, V^n + (1-\theta)\, V^{n+1}) \\ &+ c\sum_{j=1}^{2}\max\{0, \mathcal{L}_{B_j}(\theta\, V^n + (1-\theta)V^{n+1})\} \\ &+ c\sum_{j=1}^{2}\max\{0, \mathcal{L}_{S_j}(\theta\, V^n + (1-\theta)V^{n+1})\} = 0. \end{aligned} \tag{4.4}$$

We then solve (4.4) by a semi-smooth Newton iteration as in (3.10)–(3.11).

As will be described in the next subsection, the practical realization of the semi-smooth Newton iteration has to take into account the significant influence of convection induced by the buy and sell operators on the respective active sets. Stabilization is necessary even for small values of the regularization parameter $c$. In order to balance the influence of regularization error (which is small for large $c$) and of the magnitude of convection (which is small for small $c$), we found it favorable to work with moderate values for $c$.

To reduce the influence of the incurred remaining regularization error, we embed the semi-smooth Newton iteration for each time step into an Augmented Lagrangian (ALM) loop. That is, (4.4) is replaced by

$$\begin{aligned}\frac{V^{n+1}-V^n}{\tau} &+ \mathcal{L}(\theta\, V^n + (1-\theta)\, V^{n+1})\\ &+ \sum_{j=1}^{2} \max\{0, \lambda_{B_j} + c\,\mathcal{L}_{B_j}(\theta\, V^n + (1-\theta)V^{n+1})\}\\ &+ \sum_{j=1}^{2} \max\{0, \lambda_{S_j} + c\,\mathcal{L}_{S_j}(\theta\, V^n + (1-\theta)V^{n+1})\} = 0. \qquad (4.5)\end{aligned}$$

During one semi-smooth Newton loop for (4.5), the Lagrange multiplier estimates $\lambda_{B_j}$ and $\lambda_{S_j}$ remain unchanged. Once the Newton iteration for $V^n$ terminates, $\lambda_{B_j}$ and $\lambda_{S_j}$ are updated according to

$$\begin{aligned}\lambda_{B_j} &:= \max\{0, \lambda_{B_j} + c\,\mathcal{L}_{B_j}(\theta\, V^n + (1-\theta)V^{n+1})\}\\ \lambda_{S_j} &:= \max\{0, \lambda_{S_j} + c\,\mathcal{L}_{S_j}(\theta\, V^n + (1-\theta)V^{n+1})\}\end{aligned}$$

for $j = 1, 2$. At the beginning of each time step, all $\lambda_{B_j}$ and $\lambda_{S_j}$ are initialized by constant extrapolation from the previous time step. Upon termination of the Augmented Lagrangian loop in any given time step, complementarity systems similar to (3.17) for the 1D case are satisfied.

The complete Augmented Lagrangian semi-smooth Newton algorithm is given as Algorithm 4.1. We emphasize that in Augmented Lagrangian methods, it is not necessary to take the penalty parameter $c \to \infty$. In the present context, this prevents the convective terms in (4.5) from becoming overly dominant. For convergence it is sufficient that the Lagrange multiplier estimates $\lambda_{B_j}$ and $\lambda_{S_j}$ converge, and $c$ may remain fixed or increase only moderately. We refer to (Bertsekas 1996, Chapters 2–3) and (Ito and Kunisch 2008, Chapter 3) for the corresponding analysis in finite and infinite dimensional spaces, respectively.

## 4.1 Discretization in space and computational domain

The spatial discretization of the value function $V$ is based upon linear continuous finite elements. This choice offers more flexibility, e.g., with respect to local grid refinement, than does the finite difference approach. In order to assemble the weak form of $\mathcal{L}$, see (2.16a), we convert the second-order contributions in $\mathcal{L}$ into divergence form using

$$C_0 \circledast V_{yy} = \operatorname{div}(C_0 \nabla V) - \sum_{i=1}^{n} \frac{\partial C_0}{\partial y_j} \frac{\partial}{\partial y_j} V, \tag{4.6}$$

where $\circledast$ denotes the Hadamard product of matrices, i.e., $(A \circledast B)_{i,j} = A_{i,j} \, B_{i,j}$. The coefficient matrix is given by

$$(C_0)_{k,l} = \frac{1}{2} \sum_{i,j=1}^{n} A_{ij} \, y_i \, y_j (\delta_{ik} - y_k)(\delta_{jl} - y_l),$$

where $\delta_{ik}$ denotes the Kronecker delta symbol. This conversion into divergence form incurs an additional convection term, the last term in (4.6), which needs to be added to the connection terms already present in (2.16a).

In order to accomodate potentially highly convective contributions in (4.5), the discretization of the first-order terms is based upon an upwind triangle stabilization, as described for instance in (Roos et al. 1996, Chapter III, Section 3). This applies to the convective terms in $\mathcal{L}$ as well as to those in the buy and sell operators $\mathcal{L}_{B_j}$ and $\mathcal{L}_{S_j}$, see (2.16).

It is well known that for the range of problem parameters of interest, the no-trading region is small and well inside the solvency region (4.1). This was also already observed in the one-dimensional case treated in Sect. 3. Together with the fact that our main interest lies in the no-trading region and the optimal trading structure in its neighborhood, this suggests once again a restriction of the computational domain. We choose our computational domain as the diamond-shaped region

$$\mathcal{S}_{\text{red}} = \{ y \in \mathbb{R}^2 : \| y - \hat{\eta} \|_1 < R \}$$

centered around the Merton fraction, where $R > 0$ is chosen problem dependent.

The choice of boundary conditions on $\partial \mathcal{S}_{\text{red}}$ is based on the current configuration of the active sets. Since the boundary conditions are not of variational type, we adjoin them as equality constraints to the linear system (4.5) by introducing additional Lagrange multipliers. This converts (4.5) to a saddle point problem of the form

$$\begin{bmatrix} A & B^\top \\ B & 0 \end{bmatrix} \begin{pmatrix} V \\ p \end{pmatrix} = \begin{pmatrix} b \\ 0 \end{pmatrix}.$$

The rows of $B$ have, for instance, entries of the form

$$\int_{\partial \mathcal{S}_{\text{red}}} \mathcal{L}_{B_1} \, \varphi_j \, \varphi_i \, \mathrm{d}s, \quad j = 1, \ldots, n_{\text{nodes}},$$

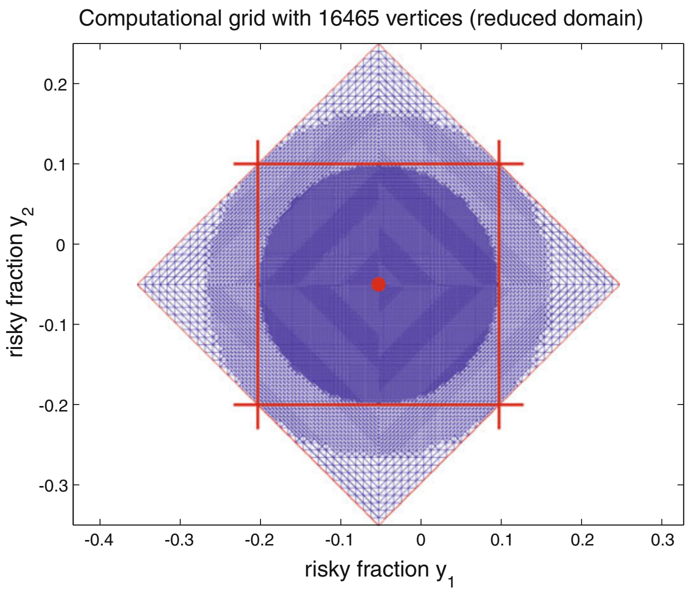


**Fig. 5** Computational grid used in Example 4.1 on the reduced domain $\mathcal{S}_{\text{red}}$ centered at the Merton fraction. The regions outside the *inner square* pertain to the assisted active set strategy (4.7). (Color figure online)

where node $i \in A_{B_1} \cap NT_2$. At parts of the boundary which belong to two active sets, we use the sum of the two contributions from each of them.

It is known that the no-trading region is enclosed to the left and the right by buy and sell regions for the first asset, and analogously on top and below by the second asset. This knowledge is used to assist the choice of active sets in Algorithm 4.1, step 9. Indeed, in practice we use

$$\begin{aligned} \widetilde{A}_k^{B_j} &:= A_k^{B_j} \cup \{y \in \mathbb{R}^2 : y_j - \hat{\eta}_j \leq -R/2\}, \quad j = 1, 2, \\ \widetilde{A}_k^{S_j} &:= A_k^{S_j} \cup \{y \in \mathbb{R}^2 : y_j - \hat{\eta}_j \geq R/2\}, \quad j = 1, 2. \end{aligned} \tag{4.7}$$

The assist strategy can be interpreted as applying boundary conditions in a penalized form in a square of side length $R$ centered at the Merton fraction which is inscribed into $\mathcal{S}_{\text{red}}$, see Fig. 5.

The graphical representation of the trading regions in the examples below is based on an inexpensive postprocessing step in which the active sets on every time level $n$ are determined according to the *unstabilized* buy and sell operators, i.e.,

$$\begin{aligned} A^{B_j} &= \{y \in \mathcal{S}_{\text{red}} : \mathcal{L}_{B_j}^{\text{unstab}} V^n > 0\} \\ A^{S_j} &= \{y \in \mathcal{S}_{\text{red}} : \mathcal{L}_{S_j}^{\text{unstab}} V^n > 0\}. \end{aligned} \tag{4.8}$$

### 4.2 Adaptive time stepping

Algorithm 4.1 is stated for a predetermined number $N$ of time steps of fixed length $\tau$. Computational experience shows that the changes in the trading regions can be highly varying in time, especially near the final time $T$. This suggests the use of an adaptive time stepping procedure. We gave preference to a simple heuristic procedure over classical ones. Our target is to choose the time step size $\tau_n$ such that

$$d_{\text{rel}} := \frac{\|\nabla(V^{n+1} - V^n)\|_{L^2(\mathcal{S}_{\text{red}})}}{\|\nabla V^n\|_{L^2(\mathcal{S}_{\text{red}})}} \approx C. \tag{4.9}$$

The new time step is chosen as $\min\{\max\{\tau_n/d_{\text{rel}},\ \tau_{\min}\},\ \tau_{\max}\}$ where $\tau_{\min} = 10^{-4}$ and $\tau_{\max} = 5 \cdot 10^{-2}$. A time step is accepted if $d_{\text{rel}}/C < 1.2$ or if $\tau_n = 10^{-4}$, and otherwise rejected. Typically, rejection only occured at the first time step when the initial $\tau$ was chosen too large.

### 4.3 Numerical results

As in the 1D case, we used the implicit Euler time-stepping scheme ($\theta = 1$) and a locally refined spatial grid near the Merton fraction for all computations. The mesh for Example 4.1 is shown in Fig. 5. It contains 32,776 triangles and 16,465 vertices, i.e., degrees of freedom in the linear systems in step 10 of Algorithm 4.1.

The iteration for any given time level $n$ of the SSN loop was terminated as soon as one the following criteria were met:

(1) the active sets coincided,
(2) jump terms analogously defined as in (3.19) were below $10^{-9}$,
(3) the relative change between iterations in the value function

$$\frac{\|V^n_{k+1} - V^n_k\|_{L^\infty(\mathcal{S}_{\text{red}})}}{\|V^n_{k+1}\|_{L^\infty(\mathcal{S}_{\text{red}})}}$$

was below $10^{-12}$.

Typically, criteria (1) or (3) were satisfied first with only very few occurences of criterion (2). This clarifies the stopping in step 8 of Algorithm 4.1.

The outer ALM loop was essential in converging the trading regions especially in the first few time steps (where time $t$ is near $T$). We found three ALM steps to be sufficient in each case.

**Algorithm 4.1** Semi-smooth Newton Augmented Lagrangian time-stepping method in the two-dimensional case

Initialize $V^N$ according to (2.15)
**for** $n = N-1, \dots, 1$ **do**
  Initialize $V_0^n := 2\,V^{n+1} - V^{n+2}$ (or $V_0^{N-1} = V^N$)
  Initialize $\lambda_{B_j,0}^n := \lambda_{B_j}^{n+1}$ (or $\lambda_{B_j,0}^{N-1} = 0$) for $j = 1, 2$, and similarly for $\lambda_{S_j}$
  Set $\ell := 0$
  **while** not converged (ALM) **do**
    Set $k := 0$
    **while** not converged (SSN) **do**
      Set

$$A_k^{B_j} := \{y \in \mathcal{S} : \lambda_{B_j,k}^n + c\,\mathcal{L}_{B_j}^{\text{stab}}(\theta\,V_k^n + (1-\theta)V^{n+1}) > 0\}, \quad j = 1, 2$$

$$A_k^{S_j} := \{y \in \mathcal{S} : \lambda_{S_j,k}^n + c\,\mathcal{L}_{S_j}^{\text{stab}}(\theta\,V_k^n + (1-\theta)V^{n+1}) > 0\}, \quad j = 1, 2$$

      and apply the assist strategy
      Solve for $V_{k+1}^n$

$$\frac{V^{n+1} - V}{\tau} + \mathcal{L}^{\text{stab}}(\theta\,V + (1-\theta)V^{n+1}) + \sum_{j=1}^{2} \chi_{A_k^{B_j}} (\lambda_{B_j,k}^n + c\,\mathcal{L}_{B_j}^{\text{stab}}(\theta\,V + (1-\theta)V^{n+1}) + \sum_{j=1}^{2} \chi_{A_k^{S_j}} (\lambda_{S_j,k}^n + c\,\mathcal{L}_{S_j}^{\text{stab}}(\theta\,V + (1-\theta)V^{n+1}) = 0.$$

      on the reduced domain, with boundary conditions as described in Section 4.1
      Increase $k$
    **end while** (SSN)
    Update the Lagrange multipliers

$$\lambda_{B_j,\ell}^n := \max\left\{0, \lambda_{B_j,k}^n + c\,\mathcal{L}_{B_j}^{\text{stab}}(\theta\,V + (1-\theta)V^{n+1})\right\}, \quad j = 1, 2$$

    and analogously for $\lambda_{S_j,\ell+1}^n$
    Increase $\ell$
  **end while** (ALM)
  Set $V^n := V_k^n$, $\lambda_{B_j}^n := \lambda_{B_j,\ell}$ and $\lambda_{S_j}^n := \lambda_{S_j,\ell}$, $j = 1, 2$
**end for**

*Example 4.1* In our first example, we used the following problem data:

| | | | |
|---|---|---|---|
| $\alpha = -0.5$ | utility exponent | $\gamma = 0.5\,\%$ | trading costs |
| $\mu = \begin{pmatrix} -1.0\,\% \\ -1.5\,\% \end{pmatrix}$ | stock trends | $\sigma = \begin{pmatrix} 0.30 & 0.05 \\ 0.05 & 0.40 \end{pmatrix}$ | stock volatilities |
| $r = 0.0\,\%$ | interest rate | | |

on the time interval $(0, 1)$. The Merton fraction is $\hat{\eta} = (-0.0531, -0.0501)^\top$, and we consider the case with liquidation costs.

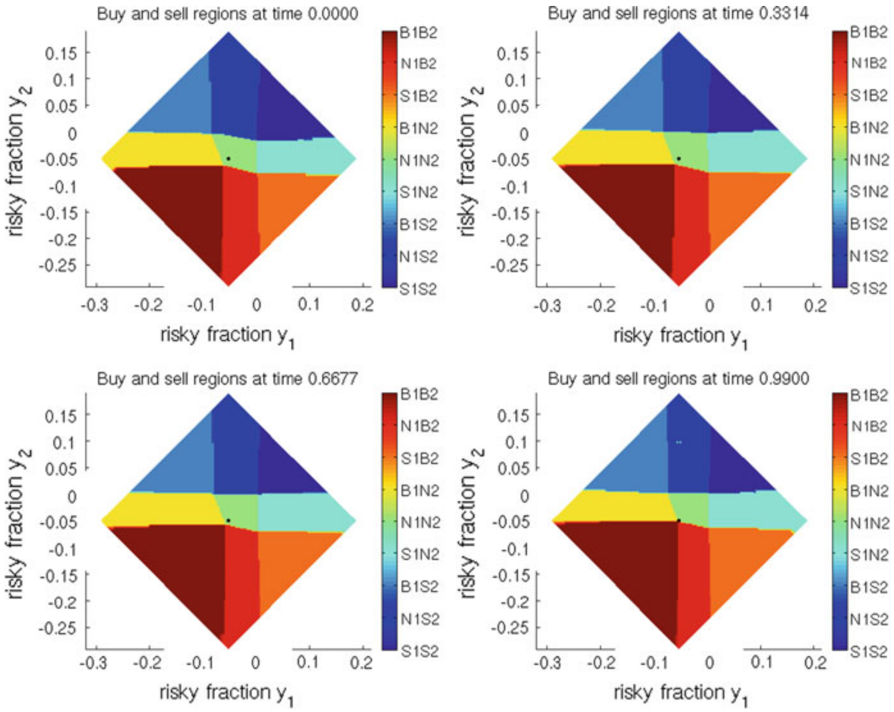


**Fig. 6** Color-coded trading regions in Example 4.1 at times near $t \in \{0, 1/3, 2/3, 1\}$. The figure shows the major part of the reduced computational domain $\mathcal{S}_{\text{red}}$ centered at the Merton fraction (*black dot*). (Color figure online)

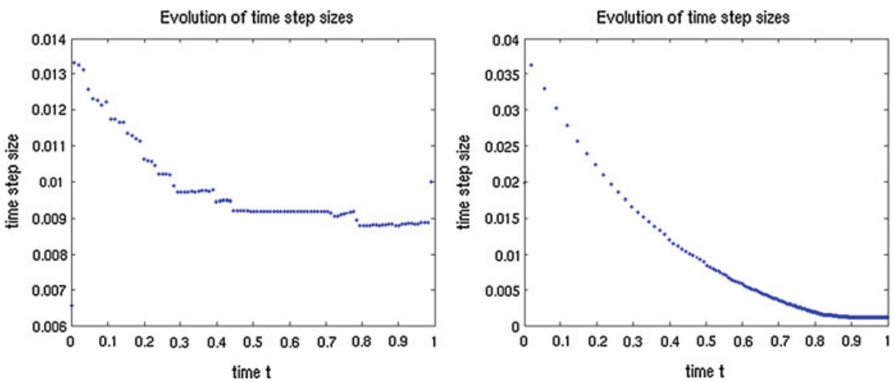


**Fig. 7** Evolution of time step sizes for Example 4.1 (*left*) and 4.2 (*right*)

We ran Algorithm 4.1 with regularization parameter $c = 10^5$ on a reduced domain of radius $R = 0.3$. With a target relative change of $\nabla V$ in between time steps of $C = 5 \cdot 10^{-3}$, see (4.9), the algorithm used 104 time steps. The evolution of time step sizes is shown in Fig. 7 (left). The nearly constant time steps reflect the relatively gentle motion of the trading regions (see Fig. 6), which is due to the utility exponent $\alpha = -0.5$, representing a high level of relative risk aversion $1 - \alpha = 1.5$. Approximately 8 semi-smooth Newton steps were used on average per time step. The total run-time was approximately 930 seconds and thus significantly higher than for the 1D problems. This is mainly due to the increased size of the linear systems in step 10 of Algorithm 4.1, which were solved using direct sparse linear algebra. To be more precise, approximately 77 % of the run-time was spent solving linear systems. These numbers can be improved by using solvers of better complexity, e.g., multigrid methods, but this is beyond the scope of this paper.

To show that our method is not restricted to the simplex we chose this example with negative trend parameters which yields a Merton fraction $\hat{\eta}$ with negative positions in the stocks (short selling of stocks). This corresponds to the one-dimensional Example 3.3. Like in that example we observe in Fig. 6 that—when approaching terminal time—the boundary of the NT-region gets closer to the Merton fraction and extends to the axes (corresponding to the red and black boundaries in Fig. 4). This is to be expected since at terminal time we have to liquidate anyway and hence can try to get closer to the Merton fraction when we are far away while this would be too expensive if our position lies 'between' Merton fraction and 0. Note that one year ($t = 0$) before terminal time we would still trade (sell stocks) when we have no position in the stocks, while at $t = 0.6677$ this is no longer optimal. This is different in the following example.

*Example 4.2* In our second example, we used the following problem data:

| | | | |
|---|---|---|---|
| $\alpha = 0.3$ | utility exponent | $\gamma = 0.5\,\%$ | trading costs |
| $\mu = \begin{pmatrix} 15.0\,\% \\ 2.0\,\% \end{pmatrix}$ | stock trends | $\sigma = \begin{pmatrix} 0.42 & 0.10 \\ 0.10 & 0.38 \end{pmatrix}$ | stock volatilities |
| $r = 7.0\,\%$ | interest rate | | |

on the time interval (0, 1). The Merton fraction is $\hat{\eta} = (1.0438, -1.0034)^\top$ in this example, and we consider again the case with liquidation costs.

We ran Algorithm 4.1 with the same algorithmic parameters as in Example 4.1, but on a reduced domain of radius $R = 4.0$. The same computational mesh (re-scaled to the new radius and centered at the Merton fraction) was used. The algorithm produced a total of 264 time steps. The evolution of time step sizes is shown in Fig. 7 (right). The increased number of time steps corresponds to the more pronounced movements of the trading regions, which relate to a lower level of risk aversion ($1 - \alpha = 0.7$). Approximately 14 semi-smooth Newton steps were used on average per time step. Consequently, the computational time was approximately three times as high (2 713 seconds) in this example. The same remarks concerning fast linear solvers as in Example 4.1 apply.

In this example the first component of the Merton fraction $\hat{\eta}$ is greater than 1 (a long position for which we have to borrow money or sell the other stock short) and the second slightly negative (short position). The shapes of the NT-regions depending on time are similar to those in the preceding Example 4.1. The interpretation close to terminal time is the same as before. But in this example it is longer optimal to trade

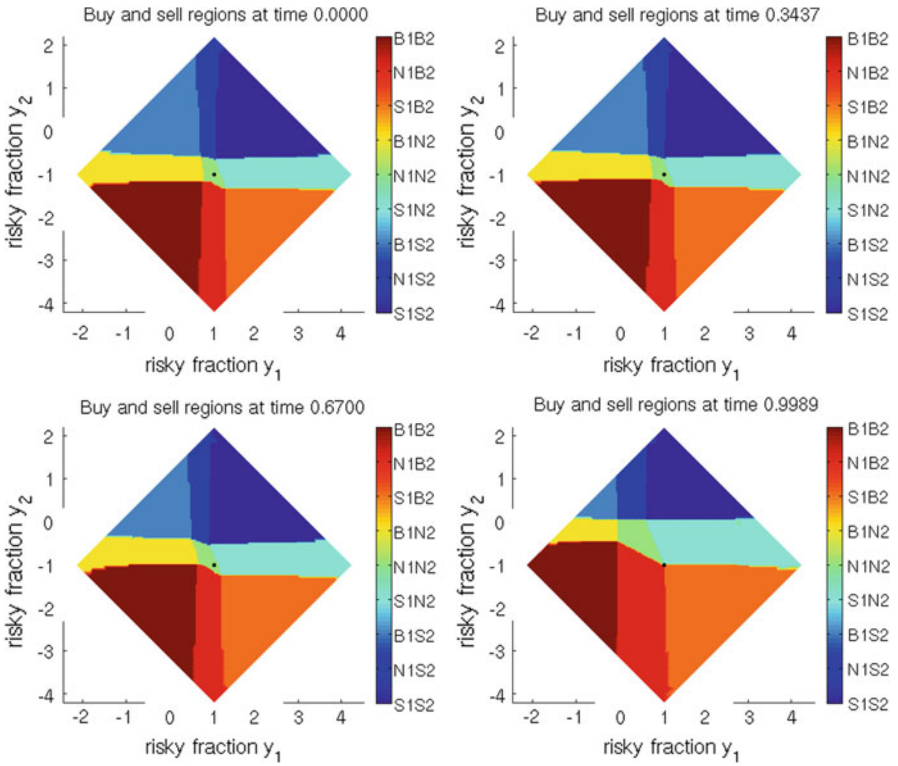


**Fig. 8** Color-coded trading regions in Example 4.2. The figure shows the major part of the reduced computational domain. It also shows the Merton fraction (*black circle*)

in the stocks when we have a position 0 in the stocks. Opposed to Example 4.1 this is true even at $t = 0.6700$ as we can see clearly from Fig. 8. This, as well as the fact that the NT-regions are smaller at the beginning when compared to Example 4.1, is due to the lower risk aversion. Moreover the NT-region is further away from 0 as a consequence of the more extreme trend parameter of the first stock yielding a more extreme $\hat{\eta}$.

## 5 Extensions

There are several model variations and extensions to which the proposed methods carry over with minor modifications. For instance, analogous results can be obtained for logarithmic utility; and more general cost coefficients, which may be different for buying and selling and may differ among assets, can be treated as well.

Instead of liquidating the position in the stocks we may maximize the expected utility of terminal total wealth, corresponding to the value function

$$\tilde{\Phi}(t, x_0, x) = \sup_{(L,M)} \mathrm{E}\left[\tfrac{1}{\alpha}\left(X_0(T) + \mathbf{1}^\top X(T)\right)^\alpha \mid X_0(t-) = x_0,\, X(t-) = x\right]$$

instead of (2.5). In Theorem 2.1 this would only change the terminal condition to $\tilde{\Phi}(T, x_0, x_1) = \frac{1}{\alpha}(x_0 + \mathbf{1}^\top x)^\alpha$. The homotheticity property (2.10) also holds for $\tilde{\Phi}$. Hence we can consider $\tilde{V}(t, y) = \tilde{\Phi}(t,\ 1 - \mathbf{1}^\top y,\ y)$ for which we have to solve (2.14) with terminal condition $\tilde{V}(T, y) = 1/\alpha$ instead of (2.15).

If neither short selling nor borrowing are allowed, we would require that the wealth processes stay positive and the total wealth strictly positive. After reducing the dimension we have to solve on $[0, T) \times \mathcal{D}$ an HJB equation based on the same operators as in Theorem 2.2 with the same terminal condition (2.15). Here $\mathcal{D}$ denotes the simplex in $\mathbb{R}^n$. On the boundary $\partial\mathcal{D}$ we have to take care which actions are not admissible and we may have to exclude the corresponding inequalities, cf. Akian et al. (1995). In that case the boundary conditions are given by the dynamics of the non-empty neighbouring region, e.g. by $V_t + \mathcal{L}V = 0$ on $\partial\mathcal{D} \cap \partial NT(t)$.

Further, we may allow for consumption. Instead of (2.3a) we would have dynamics

$$\mathrm{d}X_0(t) = rX_0(t)\,\mathrm{d}t - c(t)\,\mathrm{d}t - (1+\gamma)\,\mathrm{d}(\mathbf{1}^\top L(t)) + (1-\gamma)\,\mathrm{d}(\mathbf{1}^\top M(t)),$$

in the bank account, where $c(t) \geq 0$ is the consumption rate at $t$.

Optimizing consumption and terminal wealth, we then may consider the value function

$$\Phi(t, x_0, x) = \sup_{(c,L,M)} \mathrm{E}\left[\frac{1}{\alpha}\int_t^T c(s)^\alpha\,\mathrm{d}s + \frac{1}{\alpha}\left(X_0(T) + \mathbf{1}^\top X(T) - \gamma\,\|X(T)\|_1\right)^\alpha \middle|\, X_0(t-) = x_0,\, X(t-) = x\right]$$

instead of (2.5). This yields an additional term $\frac{c^\alpha}{\alpha} - c\,\Phi_{x_0}$ in the HJB. Inserting the maximzer $\hat{c} = \left(\Phi_{x_0}\right)^{\frac{1}{1-\alpha}}$ and performing the transformation to risky fractions then yields, instead of (2.14), the HJB

$$\max\{V_t + \tfrac{1-\alpha}{\alpha}(\alpha V - y^\top V_y)^{\frac{\alpha}{1-\alpha}} + \mathcal{L}V,\ \max_{1\leq i\leq n}\mathcal{L}_{B_i}V,\ \max_{1\leq i\leq n}\mathcal{L}_{S_i}V\} = 0,$$

where the operators and boundary conditions are the same as without consumption.

## References

Akian M, Menaldi JL, Sulem A (1996) On an investment-consumption model with transaction costs. SIAM J Control Optim 34:329–364

Akian M, Séquier P, Sulem A (1995) A finite horizon multidimensional portfolio selection problem with singular transactions. In: Proceedings of the 34th conference on decision and control, vol 3, pp 2193–2198

Almgren R, Tourin A (2004) Optimal soaring with Hamilton–Jacobi–Bellman equations (preprint). URL:http://cims.nyu.edu/~almgren/papers/optsoar.pdf

Bertsekas DP (1996) Constrained optimization and lagrange multiplier methods. Athena Scientific, Belmont

Dai M, Zhong Y (2010) Penalty methods for continuous-time portfolio selection with proportional transaction costs. J Comput Financ 13(3):1–31

Dai Min, Yi Fahuai (2009) Finite-horizon optimal investment with transaction costs: a parabolic double obstacle problem. J Differ Equ 246(4):1445–1469. ISSN 0022-0396. doi:10.1016/j.jde.2008.11.003

Davis MHA, Norman AR (1990) Portfolio selection with transaction costs. Math Oper Res 15:676–713

Evans G (1979) A second order elliptic equation with gradient constraint. Commun Partial Differ Equ 4:555–572

Griesse R, Kunisch K (2009) A semismooth Newton method for solving elliptic equations with gradient constraints. ESAIM M2AN: Math Model Numer Anal 43(2): 209–238. doi:10.1051/m2an:2008049

Hintermüller M, Kunisch K (2006) Feasible and non-interior path-following in constrained minimization with low multiplier regularity. SIAM J Control Optim 45: 1198–1221. doi:10.1137/050637480

Hodder JE, Tourin A, Zariphopoulou T (2001) Numerical schemes for variational inequalities arising in international asset pricing. Comput Econ 17:43–80

Irle A, Sass J (2006) Optimal portfolio policies under fixed and proportional transaction costs. Adv Appl Probab 38:916–942

Ito K, Kunisch K (2008) Lagrange multiplier approach to variational problems and applications volume 15 of advances in design and control. Society for Industrial and Applied Mathematics (SIAM), Philadelphia

Kunisch K, Sass J (2007) Trading regions under proportional transaction costs. In: Waldmann K-H, Stocker UM (eds) Operations research proceedings. Springer, New York pp 563–568

Li W, Wang S (2009) Penalty approach to the HJB equation arising in European stock option pricing with proportional transaction costs. J Optim Theory Appl 143(2):279–293. ISSN 0022-3239. doi:10.1007/s10957-009-9559-7

Merton RC (1969) Lifetime portfolio selection under uncertainty: the continuous-time case. Rev Econ Stat 51(3):247–257

Muthuraman K (2007) A computational scheme for optimal investment-consumption with proportional transaction costs. J Econ Dyn Control 31(4): 1132–1159. doi:10.1016/j.jedc.2006.04.005

Muthuraman K, Kumar S (2006) Multidimensional portfolio optimization with proportional transaction costs. Math Financ Int J Math Stat Financ Econ 16(2): 301–335. doi:10.1111/j.1467-9965.2006.00273.x

Roos H-G, Stynes M, Tobiska L (1996) Numerical methods for singularly perturbed differential equations. Springer, Berlin

Shreve S, Soner HM (1994) Optimal investment and consumption with transaction costs. Ann Appl Probab 4:609–692

Zakamouline VI (2005) A unified approach to portfolio optimization with linear transaction costs. Math Methods Oper Res 62(2):319–343. ISSN 1432-2994. doi:10.1007/s00186-005-0005-9